

Supplemental Materials and Methods

Northern blot

RNA was isolated from BM, spleen, and thymus of $RhoH^{+/+}$, $RhoH^{+/-}$, and $RhoH^{-/-}$ mice using the Trizol (Invitrogen, Carlsbad, CA) reagent according to the manufacturer's procedures. Northern blotting was performed according to standard protocols. RNA was detected with the probe generated from a *RhoH* subclone with the primers 5'-GCGGAATTGCTGCTGAGCTCAATCAAGTGC-3' and 5'-GCGGGATCCCTTAGAAGATCTTGCATTCATTGAT-3' recognizing the *RhoH* coding region. The membrane with RNA was stripped and sequentially reprobed for neomycin resistance cassette and GAPDH.

Quantitative RT-PCR

Wild-type DN thymocytes enriched by MACS (Miltenyi Biotec, Bergisch Gladbach, Germany) were sorted for DN1, DN2, DN3, and DN4 with FACSria (BD PharMingen, San Diego, CA). DP, CD4SP, and CD8SP thymocytes were sorted with FACSria, whereas $CD4^{+}$, $CD8^{+}$, and $B220^{+}$ splenocytes and Gr-1⁺ BM cells were enriched by MACS. RNA was isolated from sorted cell populations using the Absolutely RNA Microprep Kit (Stratagene, La Jolla, CA) and the RNeasy Mini Kit (Qiagen, Valencia, CA). One microliter cDNA, generated from 15 ng RNA using the iScript cDNA Synthesis Kit (Bio-Rad, Hercules, CA), was subjected to real-time PCR with the iQ SYBR Green Supermix (Bio-Rad) on the iCycler (Bio-Rad). Primers 5'-AGTCATTCGCACACCAGTTG-3' and 5'-AGTCTGCCCAGGTGAGAAAC-3' spanning the exon 2-exon 3 border were used. *RhoH* gene expression was quantified with the Gene Expression Analysis Program for iCycler iQ Real-Time PCR Detection System (Bio-Rad). GAPDH was used to normalize gene expression, and *RhoH* expression level in DP cells was set to 1.

Adhesion assays to ICAM-1 and VCAM-1

Adhesion assays were performed as described in "Materials and methods." Cells were resuspended in HBSS and preincubated with 2 mM EDTA, 5 mM Mg^{2+} , 1 mM Mn^{2+} , 20 ng/mL PMA, or a combination for 10 minutes at 37°C and then plated on ICAM-1 and VCAM-1. The number of adherent cells was calculated as described in "Materials and methods." Assays were performed in triplicate and repeated 4 to 8 times.

	control		RhoH ^{-/-}		
	average	stdev	average	stdev	
Bone marrow (x 10⁶ cells)					
Mac1+ Gr-1+	28,053	7,660	34,815	6,358	
Mac1+ Gr-1-	3,865	1,191	3,687	3,324	
Ter119+	6,882	2,184	8,870	3,309	
NK1.1+	0,448	0,249	0,561	0,294	
CD4+	0,717	0,381	0,398	0,241	
CD8+	0,482	0,385	0,135	0,096	
B220+IgM-	3,392	1,746	3,829	1,818	
B220+IgM+	2,361	1,323	3,043	2,005	
B220+IgM+IgD+	1,678	1,079	1,197	0,798	
Spleen (x 10⁶ cells)					
Mac1+ Gr-1+	4,420	2,637	7,150	2,565	
Mac1+ Gr-1-	9,542	4,128	7,964	4,431	
Ter119+	13,099	2,144	24,964	5,132	**
NK1.1+	4,152	3,913	3,988	2,502	
CD4+	35,980	17,154	16,754	10,400	*
CD8+	20,818	12,091	7,710	4,107	*
IgD+	59,688	32,042	71,711	34,165	
Lymph nodes (x 10⁶ cells)					
CD4+	4,114	1,992	1,171	0,493	*
CD8+	1,747	1,069	0,441	0,280	*
IgM+IgD+	1,468	0,820	1,430	1,267	

Table S1: Absolute sizes of myeloid, erythroid, and lymphoid populations in hematopoietic organs. Presented are the absolute numbers with SD of cell populations carrying indicated surface markers in single-cell suspensions of bone marrow, spleen, and lymph nodes of 6-month-old control and RhoH-null mice. *P < .05; **P < .01; n = 5/5.

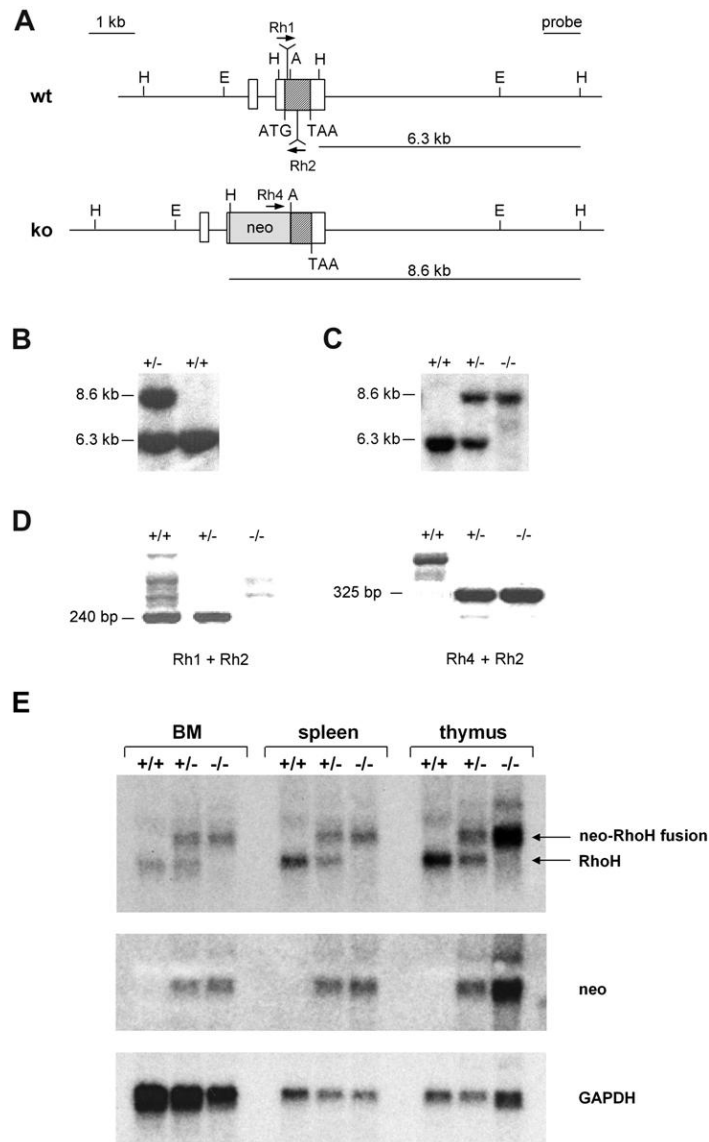


Figure S1: Generation of RhoH-deficient mice and Northern blot analysis of RhoH mutant mice. (A) Schematic presentation of the *RhoH* gene before (wild-type) and after (knockout) homologous recombination of the targeting vector (*EcoRI-EcoRI* fragment of the knockout gene). Homologous recombinants were identified by digestion of genomic DNA with *HindIII* and Southern blot hybridization with the indicated probe, resulting in a 6.3-kb fragment for wild-type and an 8.6-kb fragment for the recombined gene. Mice were genotyped using genomic PCR with forward primers specific for wild-type (Rh1) or knockout (Rh4) and a common reverse primer (Rh2). Exons are boxed, and the coding region of RhoH is hatched. neo indicates neomycin resistance expression cassette; A, *AatII*; H, *HindIII*; E, *EcoRI*; ATG, translation start site; TAA, stop codon. (B) Southern blot analysis of ES cell DNA as described in panel A, identifying homologously recombined ES cells. (C) Southern blot analysis of mouse tail DNA as described in panel A, identifying wild type (+/+), heterozygous (+/-), and homozygous (-/-) RhoH mutants. (D) Genomic PCR of mouse tail DNA as described in panel A, identifying wild type (+/+), heterozygous (+/-), and homozygous (-/-) RhoH mutants. Indicated sizes correspond to the expected sizes according to the genomic map. (E) Northern blot analysis was carried out with total RNA isolated from bone marrow (BM), spleen, and thymus of wild-type (+/+), heterozygous (+/-), and homozygous (-/-) RhoH mutant mice. The blot was hybridized sequentially with a probe for RhoH (top), neomycin resistance (neo; medium), and GAPDH (bottom). Transcripts for the endogenous RhoH mRNA (RhoH) and the neo-RhoH fusion transcript (neo-RhoH fusion) are indicated. In heterozygous animals, equal amounts of the neo-RhoH fusion and the endogenous RhoH were detected in all tissues, indicating a 50% decreased expression of the endogenous wild-type RhoH.

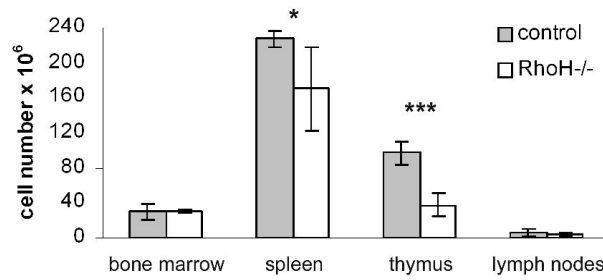


Figure S2: Decreased cellularity of thymus and spleen in the absence of RhoH. Cellularity of BM, spleen, thymus, and lymph nodes of 2-month-old RhoH-null and control mice. *P < .05; ***P < .001; n = 5/5.

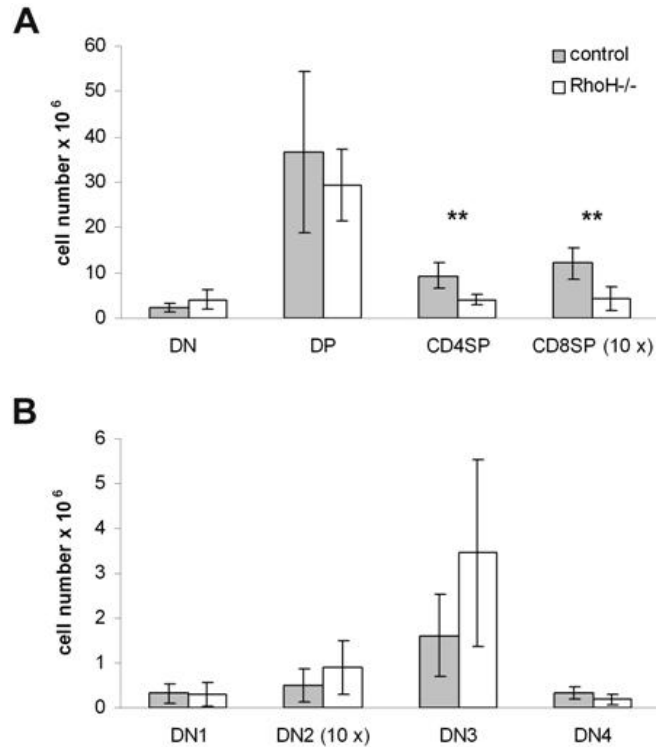


Figure S3: Impaired thymocyte development in the absence of RhoH. (A) Thymocytes of 6-month-old mice were analyzed for the expression of CD4 and CD8 by FACS. **P < .01; n = 5 of 5. (B) Thymocytes of 6-month-old mice were gated for lineage-negative (B220, CD4, CD8, NK1.1, Mac1, Gr-1, Ter119) cells and analyzed for the expression of CD25 and CD44. DN1 (CD25⁻CD44⁺); DN2 (CD25⁺CD44⁺); DN3 (CD25⁺CD44⁻); DN4 (CD25⁻CD44⁻); n = 4/4.

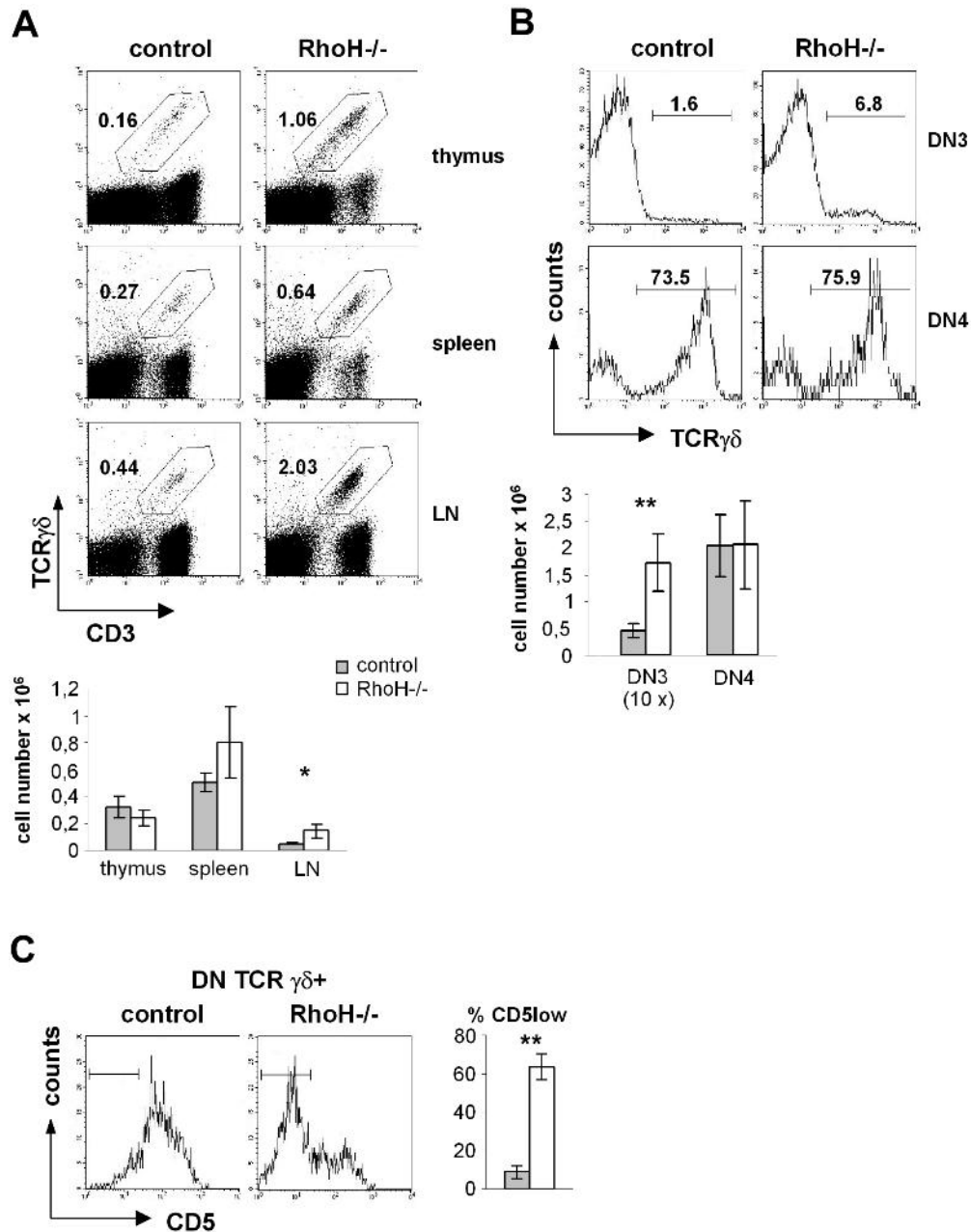


Figure S4: RhoH is not required for the development of $\gamma\delta$ T cells. (A) Single-cell suspensions of thymus, spleen, and lymph node (LN) were analyzed by FACS for the expression of TCR $\gamma\delta$ and CD3. Total cell numbers of TCR $\gamma\delta$ -expressing cells (TCR $\gamma\delta$ ⁺ CD3⁺) are shown. RhoH-null mice had normal numbers of $\gamma\delta$ T cells in thymus and spleen and increased levels in LN. *P < .05; n = 3 of 3. (B) In the absence of RhoH, the amount of TCR $\gamma\delta$ -expressing DN4 cells was unaltered, whereas the small population of TCR $\gamma\delta$ ⁺ DN3 cells was significantly elevated in RhoH-null mice. Bar graph presents the absolute numbers of TCR $\gamma\delta$ -expressing cells in the DN3 and DN4 populations. **P < .01; n = 4 of 3. (C) RhoH-null DN thymocytes showed a significantly increased percentage of CD5^{low} cells. Percentages of cells marked in histograms are shown. **P < .01; n = 2/2.

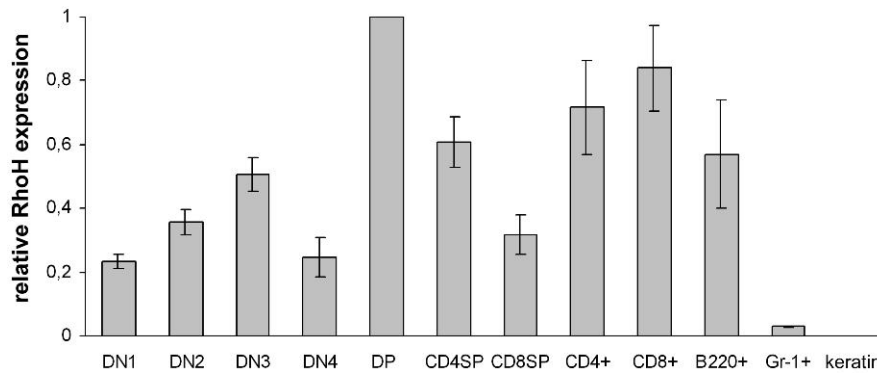


Figure S5: RhoH is expressed at all stages of T-cell development. Relative expression of RhoH was determined by qRT-PCR of total RNA isolated from sorted DN1, DN2, DN3, DN4, DP, CD4SP, CD8SP, splenic CD4⁺, CD8⁺, B220⁺, and BM Gr-1⁺ cells, as indicated. RhoH was expressed in thymocytes at all developmental stages, in mature B (B220⁺) and T (CD4⁺, CD8⁺) cells but was only weakly expressed in granulocytes (Gr-1⁺) and not detectably expressed in keratinocytes (keratin). GAPDH was used as a reference gene to normalize RhoH gene expression. RhoH expression level in DP cells was set to 1. Shown are results of 4 real-time PCR reactions performed with cDNA generated from RNA from cells of 2 independent sorts.

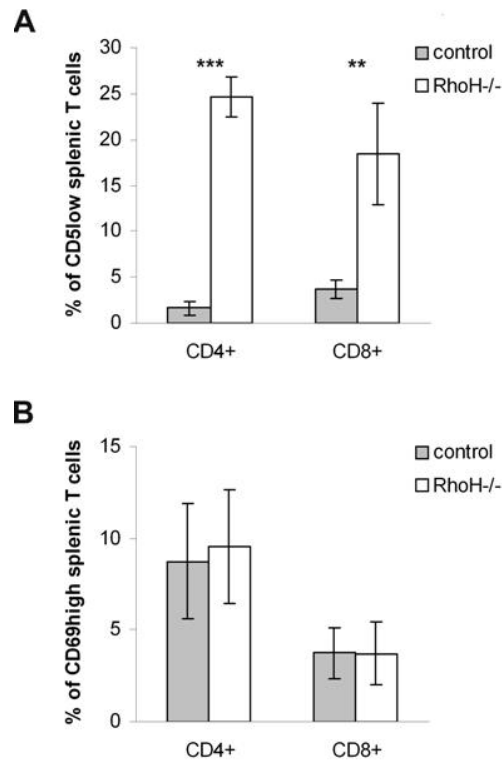


Figure S6: Decreased expression of maturation markers in RhoH-null splenocytes. (A-B) Splenocytes of 4- to 8-week-old mice were analyzed for the expression of CD4, CD8, and CD5 (A; n = 5 of 4), or CD69 (B; n = 7 of 7) by FACS. Percentages of cells marked in histograms are shown. **P < .01; ***P < .001.

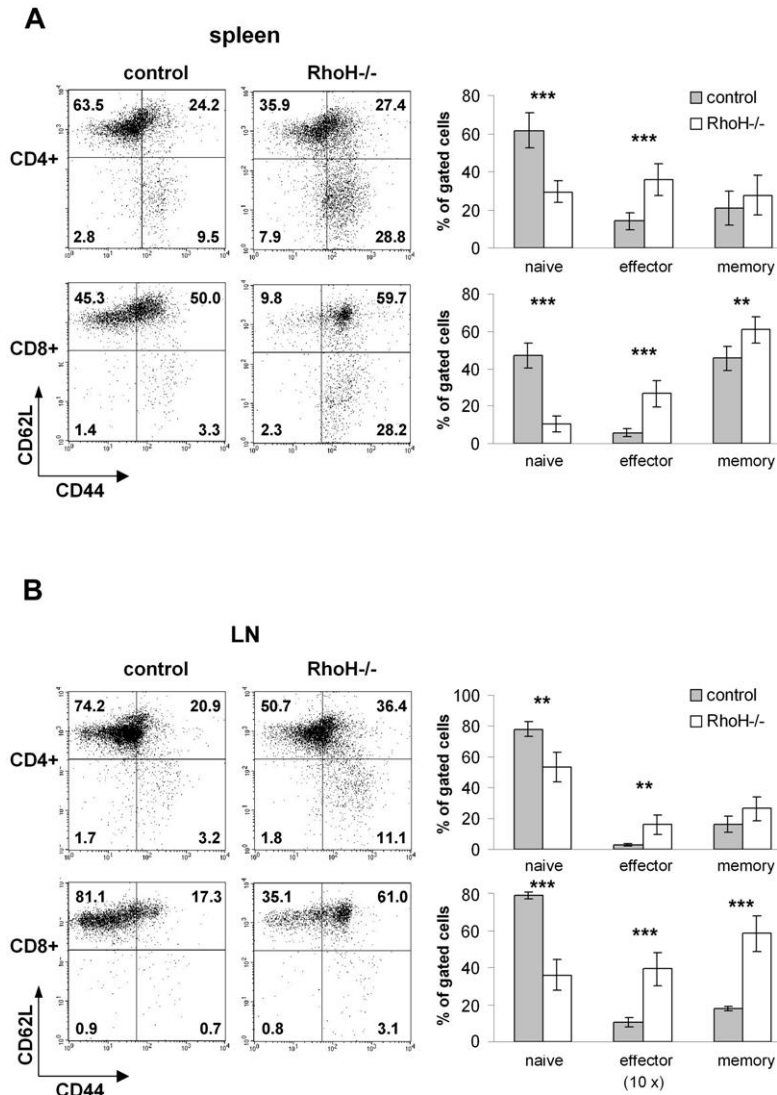


Figure S7: Reduced amounts of naïve peripheral T cells. (A-B) Splenocytes (A) and lymph node cells (B) of 4- to 8-week-old mice were analyzed for the expression of CD4, CD8, CD62L, and CD44 by FACS. In the absence of RhoH, the percentages of naïve cells (CD62L^{high}CD44^{low}) were decreased, whereas the relative amounts of effector cells (CD62L^{low}CD44^{high}) and CD8⁺ memory cells (CD62L^{high}CD44^{high}) were increased. Percentages of cells marked in histograms are shown. **P < .01; *P < .001. (A) n = 7 of 7. (B) n = 4/4.**

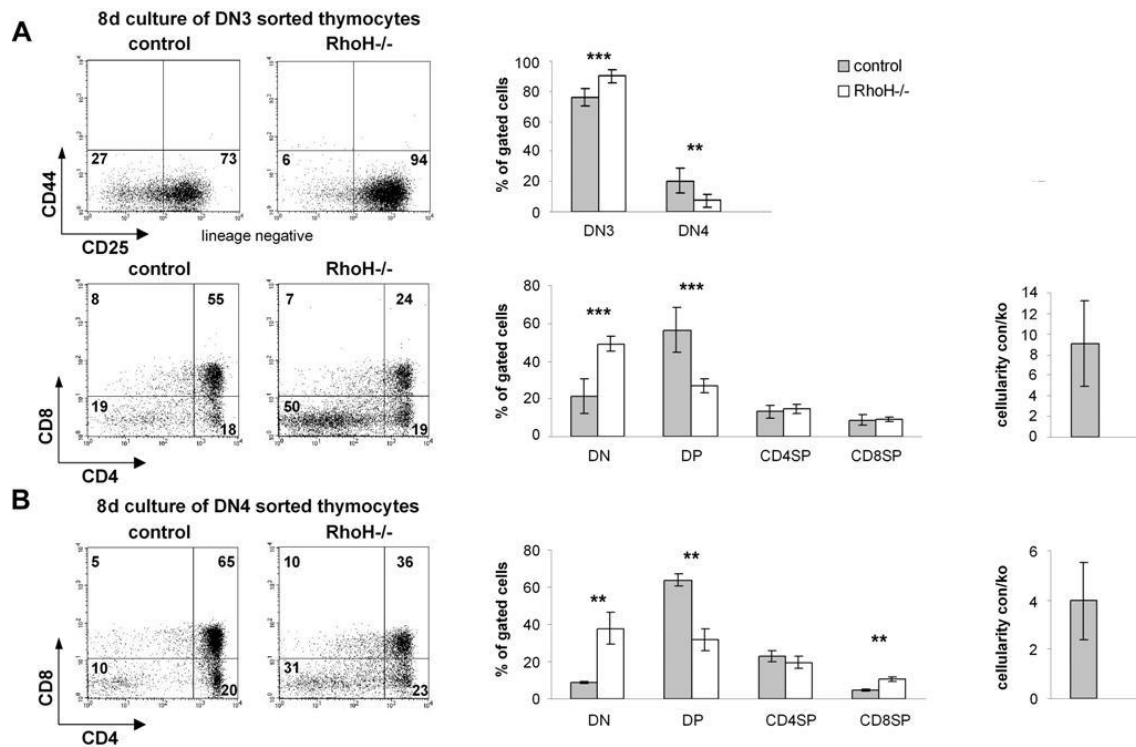


Figure S8: Impaired differentiation of RhoH-null DN3 and DN4 cells in vitro. (A) Sorted DN3 cells were cultured for 8 days on OP9-DL1 cells in the presence of IL-7 and Flt3 ligand. Differentiation from DN3 to DN4 was tested by FACS analysis of lineage-negative cells for the expression of CD44 and CD25. RhoH-null cells showed a significantly higher percentage of DN3 and a lower percentage of DN4. FACS staining for CD4 and CD8 revealed significantly increased levels of DN and reduced levels of DP in the absence of RhoH. Cellularity of the RhoH-null cultures was decreased approximately 9-fold, indicating defective expansion in the absence of RhoH. **P < .01; ***P < .001; n = 5 of 6. (B) Sorted DN4 cells were cultured for 8 days on OP9-DL1 cells in the presence of IL-7 and Flt3 ligand. FACS staining for CD4 and CD8 revealed significantly increased levels of DN and reduced levels of DP in the absence of RhoH. Furthermore, cellularity of the RhoH-null cultures was decreased approximately 4-fold, indicating defective expansion in the absence of RhoH. **P < .01; n = 3/3.

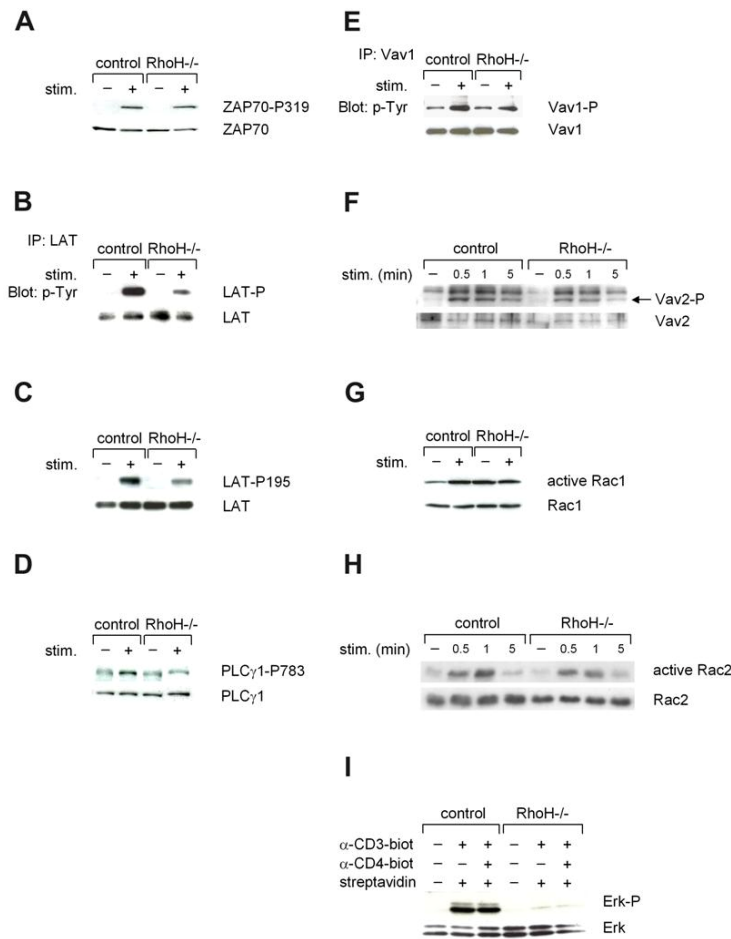


Figure S9: Defective TCR signaling in the absence of RhoH. DP thymocytes of 4- to 8-week-old mutant mice were sorted by FACS or MACS microbeads. TCR signaling was induced as indicated by cross-linking of biotinylated CD3 and CD4 antibodies with streptavidin for 5 minutes (A-E, I), 30 seconds (G), or indicated times (F, H) at 37°C. Total lysates were analyzed by Western blot for ZAP70-P319 and ZAP70 (A), LAT-P195 and LAT (C), PLCγ1-P783 and PLCγ1 (D), Vav2-P and Vav2 (F), and Erk-P and Erk (I). Immunoprecipitation (IP) for LAT (B) and Vav1 (E) was blotted with antiphosphotyrosine antibodies and reprobed with LAT (B) or Vav1 (E). Amounts of active Rac1 and Rac2 were determined by pull-down assays (G, H). Representative examples of the Western blots are shown (quantification in Figure 6).

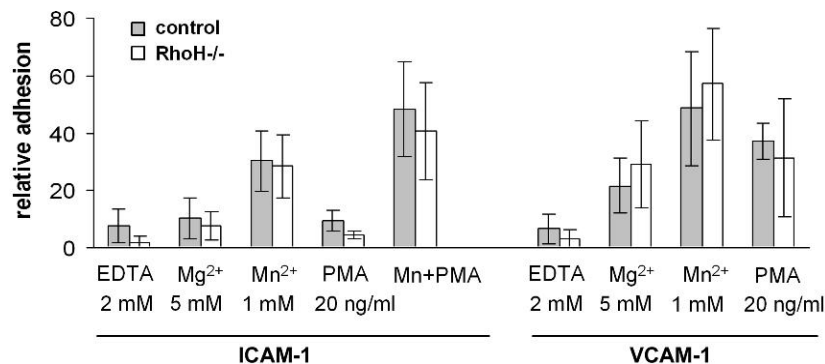


Figure S10: Normal adhesion of RhoH-null thymocytes to ICAM-1 and VCAM-1. Relative adhesion of thymocytes from 4- to 8-week-old mice to the immobilized αL³2 ligand ICAM-1 and to the αV³1 ligand VCAM-1 is shown. Nonspecific interaction was determined in the presence of EDTA. Different extents of integrin activation were achieved by treatment with Mg²⁺, Mn²⁺, PMA, Mn²⁺, and PMA (ICAM-1 EDTA, n = 6/6; Mg, n = 8/8; Mn, n = 8/8; PMA, n = 4/4; Mn+PMA, n = 8/7 and VCAM-1 EDTA, n = 6/6; Mg, n = 8/7; Mn, n = 8/7; PMA, n = 4/4).